INT. J. BIOL. BIOTECH., 17 (3): 531-541, 2020.

PHASE SYNCHRONIZATION ANALYSIS OF SENSORIMOTOR CORTEX ELECTROENCEPHALOGRAMS FOR CHANNELS C3 AND C4

Rizwan Ur Rehman[1,2], Jahangir Muhammad[1,2], Sitwat Qureshi[3], Tanweer Iqbal[4], Imran Siddiqui[1] and Syed Zeeshan Abbas[1]

[1]*Departmnt of Physics, University of Karachi, Main University Rd, Karachi75270, Sindh Pakistan*
[2]*Department of Physics, Govt. National College 1, Shaheed-e-Millat Rd., Karachi, Sindh Pakistan*
[3]*Department of Physics, Federal Urdu University of Arts, Science and Technology, University Rd, Block 9 Gulshan-e-Iqbal, Karachi, Sindh, Pakistan*
[4]*Institute of Space and Planetary Astrophysics, University of Karachi, Main University Rd, Karachi-75270, Sindh, Pakistan*

ABSTRACT

Electroencephalograms (EEG) are electrical brain maps which arise as a result of neuronal activity occurring in the cortical region of human brain. These EEG signals on the scalp surface associated with cognition and motor response of brain and are a useful guide to study human behavior and its association with the underlying brain dynamics. Appearance of EEG activity as a result of some specific cognitive or motor event is an event-related activity and associated potential is known as Event-Related-Potential (ERP). Sensorimotor process related to motor activity or sensor recognition involving multiple cortical regions of the brain is the most critical and complex brain activity. To study such inter-related cortical excitations, we present event-related-synchronization (ERS) and event-related desynchronization (ERD) analysis of motor hand movement activity paradigm conducted 10 healthy human subjects. A predefined trial sequence is presented to the subjects and EEG signals are recorded on primary motor area C3, C4 are obtained in a non-invasive manner. Phase synchronization of recorded EEG signals at channels C3, C4 are determined. High phase coherence is observed for left hand movement on C3, C4 contralateral electrodes with a correlation coefficient of 0.6922 and for right hand movement correlation coefficient is 0.6561. EEG signals on two electrodes remain phase locked for duration of 300 – 500 ms. Spectral analysis reveals spectral band in alpha rhythm (8-13 Hz), for average values of frequency with 11.613 Hz for left-hand movement and 11.305 Hz for right-hand movement. EEG signals at other electrode positions show less or no phase synchronization for hand movement motor execution paradigm.

Key words: BCI, Synchronization, EEG, NIM, Brain

INTRODUCTION

Brain electrical signals generated as a result of motor neuron activity are closely related to interconnected disciplines such as neuro-medicine, neuroscience, physics of nonlinear phenomenon and engineering. Further-more, there is a close connection between motor and cognitive activity of human brain and their associated disorders. Awareness of these interconnected problems and their detection, quantification and classification are necessary in neurorehabilitation of post-stroke patients facing brain disorders Stoykov and Madhavan (2015). Additionally, understanding of motor-activity is also useful in applied research areas related to brain control of prosthetic devices, robotic systems and vehicles. In general, Brain-Machine Interfaces (BMIs) or Brain-Computer interface (BCIs) provide a communication link between brain and external devices McFarland and Wolpaw (2008), Wolpaw *et al*. (2002), Chaudhary *et al*. (2016), Lebedev and Nicolelis (2017). A relationship between cognitive and motor activity of brain with an appearance of rhythmic neuronal signature in the sensorimotor cortex, that is, alpha rhythm (8–14 hertz) is a biological feature characterizing motor related brain activity. Brain electrical signal or electroencephalogram (EEGs) are recorded by placing electrodes on the subject's scalp and are asked to perform specific motor related tasks. Traditionally, electroencephalograms are explored using time-frequency analysis Yang *et al*. (2016), Akin (2002), spatial analysis such as Independent Component Analysis (ICA) Iriarte *et al*. (2003). Though these methods are frequently being applied on EEG data and are well known for their capability to reveal features embedded in recorded EEGs, nevertheless, are unsatisfactory in classification and association of recorded motor related brain patterns with various interconnected somatosensory cortical regions of brain. In depth understanding of the mechanism for underlying neuronal dynamics and inter relationship between motor related and cognitive activity, event-related-synchronization (ERS) and event-related-desynchronization (ERD) of alpha rhythm in sensorimotor cortex must be studied. ERD is important in understanding the decrease in spectral power density in a corresponding frequency band Delorme *et al*. (2002). Authors used cross coherence method to perform time-frequency analysis for the discrimination of EEG signals on channels Fp1, Fp2, on O1, O2 and on P3, P4, Pz. Andrew *et al*. (2017) studied the multiple cortical regions during sensorimotor activity and found strong coupling between excited regions. Ronak *et al*. (2018) investigated time-varying electroencephalograms originating at different locations on the scalp and found that these time-varying signals show correlation in terms of the physical placement of electrodes on the scalp surface. Wang *et al*. (2012) used phase synchronization technique to assess functional connectivity of multichannel neural signals. Authors concluded that phase coherence studies are more suitable in case of EEG signals recorded at low sampling rate. Quiroga *et al*. (2002) proposed a method of studying event synchronization and time-delay between EEG signals. Authors applied the proposed algorithm of EEG rat data. Algorithm was applied to intra-cranial human EEG recordings related epileptic seizure and found that it is useful in the detection of epileptic centers. Reed *et al*. (2007) studied transient neural assemblies using phase synchronization with signals obtained at specific frequencies and showed an improvement in localization of the phase synchrony. Jahangir *et al*. (2017) used Independent Component Analysis (ICA) for feature extraction and localization related to motor related brain signals. Kroupi *et al*. (2013) investigated EEG correlates of olfactory EEG signals. Authors concluded that odor-based classification of EEG signals is possible but requires rigorous analysis of pleasantness EEG data. Guger *et al*. (1999) investigated real-time left- and right-hand movement imagination EEG data and used it to control electrical devices in Brain-Computer Interface paradigm. Handayani *et al*. (2018) investigated coherence and phase synchronization in EEG data obtained for subjects with mild cognitive impairment, that is, an early stage Alzheimer's disease (AD). The study concluded that coherence and phase synchronization technique is useful in detection of early stage AD.

MATERIALS AND METHODS

EEG recordings are performed using 19 channels EEG NeuroPro 32 device with a sampling rate of 200 Hz. Each experimental session, comprising of preparation, EEG electrode placements on the scalp, and EEG data gathering takes ca. 60 minutes for one subject. Electrodes are placed on subject scalp using a 10-20 international system of electrode placements Homan *et al*. (1987). The left and right earlobes are marked as reference with A1 and A2 electrodes attached with earlobes and electrode Fz is used as common ground for other electrodes. Electrodes Fp1, Fp2, F7, F3, F4, F8, T7, C3, Cz, C4, T8, P7, P3, Pz, P4, P8, O1, O2 are mounted on the scalp surface as data gathering electrodes. Recorded data on 18 electrodes is filtered using a band pass filter in a frequency range of lying between 0.5 - 30 Hz. The experiment is performed at Neuro-Physics and Intelligence Modeling Research Laboratory, Department of Physics, University of Karachi, Karachi, Pakistan.

Participants

In the present study ten healthy subjects (5 male and 5 female) participated with an average age of 22.4 years (19 - 32 year). Participating subjects have no neurological disorder and some of the participants use eyesight glasses for vision correction during EEG data recording. Prior to experimental participation, subjects are required to give a written consent as per ethical requirement of World Medical Association Declaration of Helsinki (2001). Experimental paradigm followed in the study is explained to subjects. In order to avoid any discomfort during experiment, subject is seated on a comfortable chair with arm rests and is asked to minimize physical movements and eye blinks.

Experimental Paradigm

Experimental paradigm consists of random left- and right-hand motor execution based on an adopted trail structure presented to the participating subjects on a power point slide show. Trial structure is of 11 seconds length, structured as 4 secs resting state, 2 secs long fixation-cross and 5 secs long activity-cue of random left- and right-hand motor execution. Eleven trials per subject are recorded in one session and 4 sessions are conducted for each subject as illustrated in Figure 1. Length of each session is 121 seconds with a total of 4 x 121 seconds duration of recorded EEG data.

4 seconds	2 seconds	3 seconds
Rest	Target	Action

Fig. 1. Illustration of experimental paradigm.

Independent Components Analysis

Independent Component Analysis (ICA), just like Principal Component Analysis (PCA), is a class of blind source separation (BSS) technique. It separates a given set of signal mixture into a new set of the signals without using any information about the properties of signal. ICA is widely used in areas such as Image Processing, Speech recognition, Telecommunication, Stock Market predictions, and in particular is well suited to analyses of recorded EEG data. Besides spatial localization of brain activity from blurred mixture of signals picked up by EEG electrodes (for example to separate oscillatory activity associated with left and right hemispheric mu rhythms) present in the recorded EEG data, ICA is also used to identify and separate artifacts such as EMG (electromyogram) or EOG (electro-oculogram) activity present in EEG data. In contrast to PCA which extracts components that are merely uncorrelated, ICA separates signal mixtures into its independent components Junfeng *et al*. (2012). In order to decompose the recorded brain pattern into specific EEG signals corresponding to some cued activity, a method is devised to decompose multi-electrode EEG recorded data into static independent components Nunez *et al*. (1997). In this method 'n' linear mixtures $x_1,x_2,x_3,...,xn$ are experimentally observed from 'n' independent sources $s1,s2,s3,...,sn$ as:

$$xi = a1s1 + a2s2 + a3s3 + ... + ansn \qquad (1)$$

Where, s_i are independent components and a_{ij} are weights; they are unknown and are obtained by projecting 'n' linear experimental mixtures x_i. It can be represented in matrix form as,

$X = HS$ (2)

$$W \cong H^{-1} \quad (3)$$

The resulting equation becomes,

$$Y = WX = W(HS) = S' \cong S \quad (4)$$

The condition for ICA is that the original data from the source $s_1, s_2, s_3,..., s_n$ at any instant of time be statistically independent and the mixing of sources be linear.

Cross Coherence

The constancy between phase differences of two, time dependent signals is referred as coherence. Its value is between zero and one, if the phase difference is constant throughout the two time dependent signals then coherence is 1, it becomes 0 for random value of phase difference, it determines the functional connectivity between multi-electrodes brain signals, synchronization shows the relation between EEG signals Sankari *et al*. (2011). Cross coherence is the ratio of square of cross spectrum of two signals and the product of power spectral densities (PSD) of individual signals given by the following equation. Coherence was calculated for channels C3 and C4.

$$C_{xy}(f) = \frac{|W_{xy}|^2}{W_x(f)W_y(f)} \qquad (5)$$

Here, W_{xy} shows the cross spectral density related to two signals, f represents the frequency, W_x shows the power spectral density related to signal x and W_y shows the power spectral density related to signal y.

RESULTS AND DISCUSSION

In the present study, authors measured power spectrum of event related tasks for left- and right-hand motor execution, the left-hand motor execution is recorded on channel C4 located at right hemisphere of brain, where the right-hand execution is recorded on channel C3 located at left hemisphere of brain. The power spectrum related to channel C4 and their corresponding IC components of all subjects who have performed left-hand execution is shown in Table 1.

Table 2 shows the power spectrum related to channel C3 and their corresponding IC components of all subjects who have performed right hand motor execution. Both the tables are showing the high values of power on channel C3 for right-hand motor execution and high values of power on channel C4 for left-hand motor execution, their corresponding independent components are also showing high values of power as compare to other independent components with in active frequency range, these results are in agreement of previous research work published by Sivakami and Devi (2015).

Table 1. power spectrum for left hand activity channel C4 with independent component.

Subject	Frequency (Hz)	Channel(C4) Power (μV^2/Hz)	IC Power (μV^2/Hz)
Sb1	12	14.63	6.836(IC7)
Sb2	10	12.85	2.699(IC7)
Sb3	13	16.89	6.636(IC6)
Sb4	10	14.49	8.363(IC8)
Sb5	13	15.07	8.376(IC10)
Sb6	12	17.84	10.58(IC14)
Sb7	10	14.94	8.636(IC9)
Sb8	12	15.33	8.634(IC10)
Sb9	13	15.78	7.655(IC6)
Sb10	8	15.63	8.434(IC8)

Table 2. power spectrum for right hand activity channel C3 with independent component.

Subject	Frequency (Hz)	Channel(C4) Power (μV^2/Hz)	IC Power (μV^2/Hz)
Sb1	12	13.38	6.565(IC10)
Sb2	10	13.3	4.575(IC3)
Sb3	13	14.92	8.122(IC18)
Sb4	14	11.06	3.565(IC13)
Sb5	13	15.06	7.811(IC3)
Sb6	11	15.94	9.566(IC3)
Sb7	12	19.67	12.4(IC4)
Sb8	11	13.04	6.25(IC10)
Sb9	9	11.97	4.398(IC13)
Sb10	12	16.09	9.837(IC3)

In Fig. 2, slight peak is observed in the IC power spectra, showing that left-hand motor execution is taking place around 12 Hz performed by subject 1. The corresponding IC7 located at the right brain hemisphere on primary motor cortex of the brain region showing the left-hand motor execution, it has maximum power in all mentioned components. In Figure 3 a slight peak is observed in the IC power spectra, showing that right-hand motor execution is taking place around 10 Hz performed by subject 1. The corresponding IC17 located at the left brain hemisphere on primary motor cortex of the brain region showing the right-hand motor execution, it has maximum power in all mentioned components.

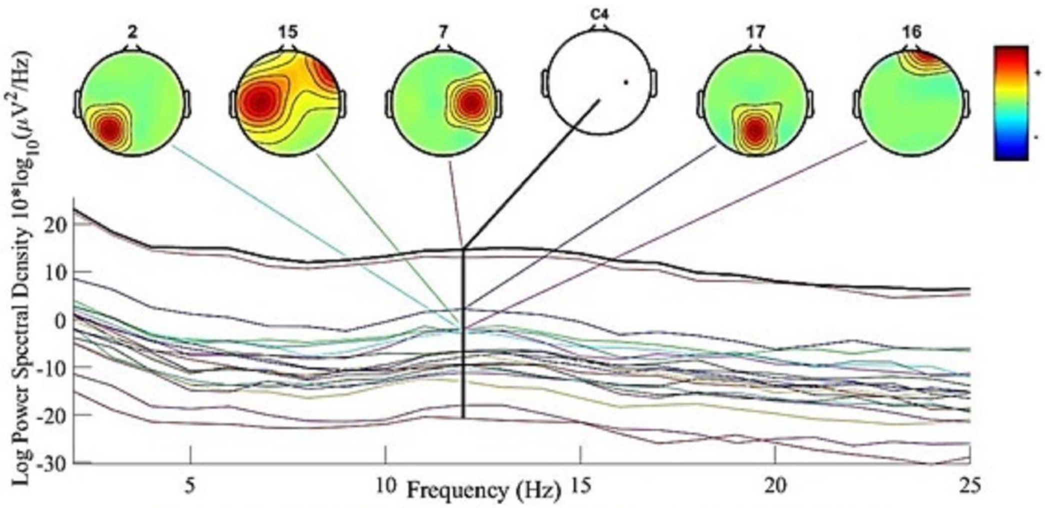

Fig. 2. Left hand movement components power spectra of subject1.

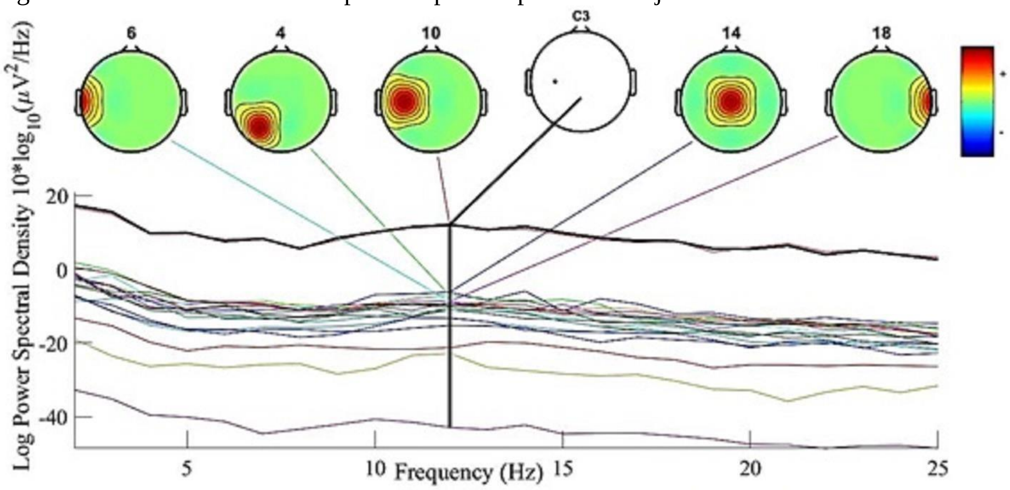

Fig. 3. Right hand movement components power spectra of subject 1.

The time frequency analysis of channel C4 for left-hand motor execution and channel C3 for right-hand motor execution performed by subject 1 is shown in Fig. 4. In the graph channel C4 for left-hand motor execution is showing activity around 12 Hz at latency around 2130 ms and a phase difference of around -13.6^0 can be easily seen between these two electrodes, where the phase is locked for 120 ms from latency 2130 ms to 2550 ms, alternatively channel C3 for right-hand motor execution is showing activity around 11.5 Hz at latency around 1930 ms and a phase difference of around -98^0 can be seen between these two electrodes, where the phase is locked for 570 ms from latency 1930 ms to 2500 ms.

Similarly, time frequency analysis of channel C4 for left-hand motor execution and channel C3 for right hand motor execution performed by subject 3 is shown in Fig. 5. In the graph channel C4 for left-hand motor execution is showing activity around 13 Hz at latency around 2050 ms and a phase difference of around -144^0 can be easily seen between these two electrodes, where the phase is locked for 285 ms from latency 2050 ms to 2335 ms, where channel C3 for right-hand motor execution is showing activity around 13 Hz at latency around 2080 ms and a phase difference of around -115^0 can be seen between these two electrodes, where the phase is locked for 220 ms from latency 2080 ms to 2300 ms.

In the same manner, time frequency analysis of channel C4 for left-hand motor execution and channel C3 for right-hand motor execution performed by subject 8 is shown in Figure 6. In the graph channel C4 is showing activity around 12 Hz at latency around 3760 ms and a phase difference of around -84^0 can be easily seen between these two electrodes, where the phase is locked for 90ms from latency 3760 ms to 3850 ms, where channel C3 for right hand is showing activity around 12 Hz at latency around 2010 ms and a phase difference of around -67^0 can be seen between these two electrodes, where the phase is locked for 160 ms from latency 2010ms to 2170 ms.

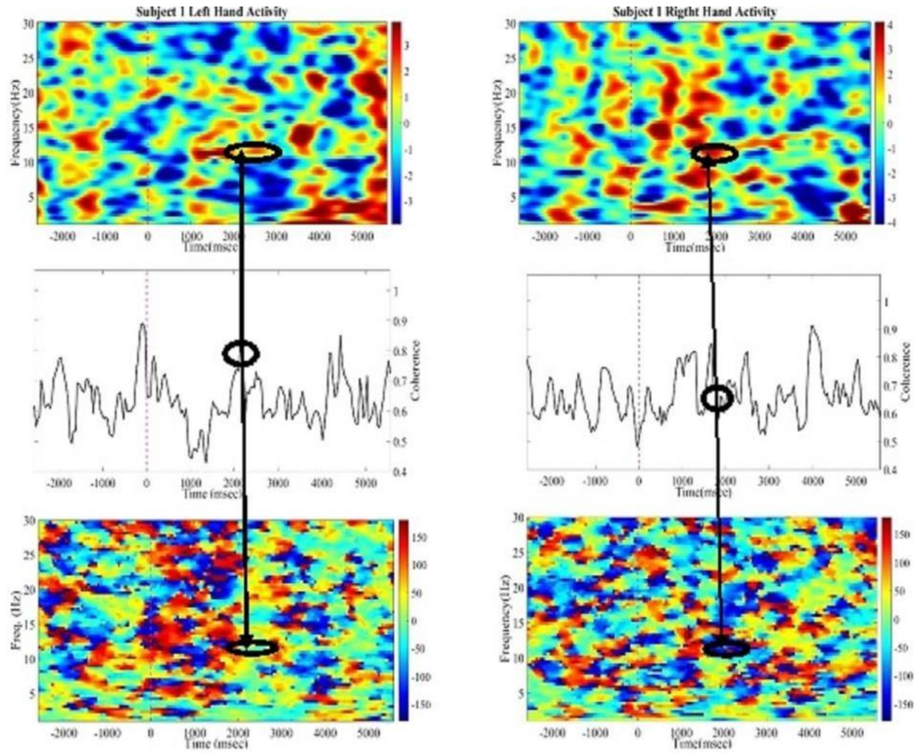

Fig. 4. Subject1 left hand and right hands activity, time frequency graph and phase coherence.

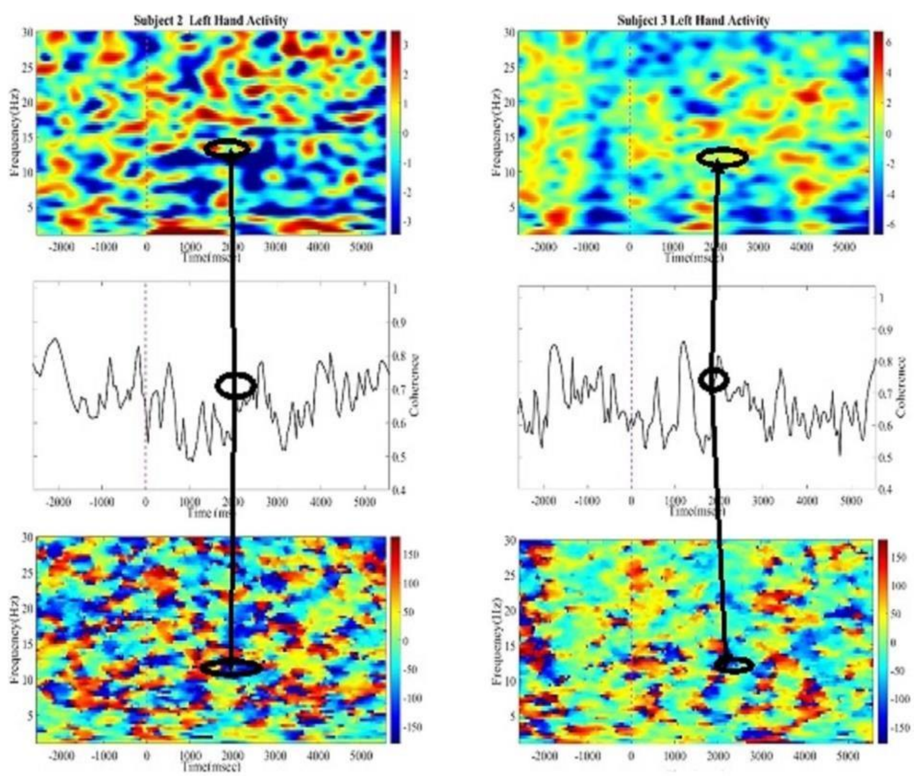

Fig. 5. Subject3 left hand and right hands activity, time frequency graph and phase coherence.

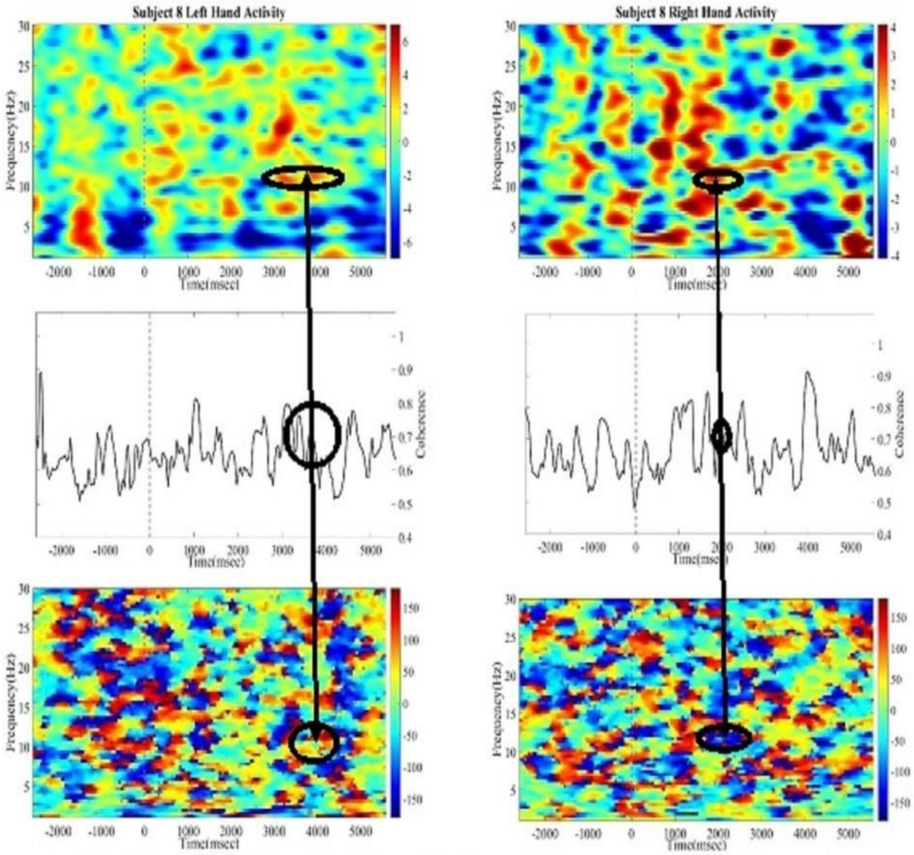

Fig. 6. Subject8 left hand and right hands activity, time frequency graph and phase coherence.

Table 3. Active frequency and related coherence of electrode pairs during left hand activity

Subject	Latency (msec)	Frequency (Hz)	F3-F4	C3-C4	P3-P4	O1-O2
Sb1	2130	12	0.6251	0.8002	0.5727	0.6837
Sb2	4010	10	0.9376	0.7237	0.8912	0.6527
Sb3	2050	13.5	0.7189	0.7245	0.547	0.5979
Sb4	3400	8.28	0.6150	0.6915	0.5881	0.6227
Sb5	3110	12.5	0.6803	0.7967	0.5598	0.6536
Sb6	4420	12.25	0.5722	0.5575	0.6054	0.6378
Sb7	4090	8.5	0.5821	0.7389	0.7475	0.5266
Sb8	3766	12.6	0.6490	0.6344	0.7842	0.5871
Sb9	3645	13	0.7744	0.6519	0.806	0.6211
Sb10	3455	13.5	0.6684	0.603	0.6008	0.7087

Table 3 is showing the latency, active frequency and comparative coherence for electrode pairs F3-F4, C3-C4, P3-P4 and O1-O2 for left-hand motor execution. Coherence of electrodes pair C3-C4 has the highest value of coherence in all other electrode pairs for all the subjects performed the activity.

Table 4 is showing the latency, active frequency and comparative coherence for electrode pairs F3-F4, C3-C4, P3-P4 and O1-O2 for right-hand motor execution. The analysis resulting that coherence of electrodes pair C3-C4 has the highest value of coherence in all other electrode pairs for all the subjects performed the activity similarly as the left-hand motor execution.

Table 5 depicts the statistical results of left-hand motor execution, the mean coherence of electrode pair C3-C4 has the highest value in all the electrode pairs. Standard deviation and standard error are also given in the table.

Table 6 depicts the statistical results of right-hand motor execution, the mean coherence of electrode pair C3-C4 has the highest value in all the electrode pairs. Standard deviation and standard error are also given in the table.

Table 4. Active frequency and related coherence of electrode pairs during right hand activity

Subject	Latency (msec)	Frequency (Hz)	F3-F4	C3-C4	P3-P4	O1-O2
Sb1	1928	11.5	0.601	0.6542	0.4841	0.6475
Sb2	2500	10.25	0.7919	0.7516	0.7478	0.7323
Sb3	2580	13	0.5135	0.7381	0.5872	0.6672
Sb4	3195	12.25	0.5823	0.5126	0.7053	0.5305
Sb5	4010	12	0.0.5337	0.639	0.5252	0.6501
Sb6	3560	10.25	0.7321	0.7405	0.6917	0.6062
Sb7	3970	10.25	0.5735	0.5442	0.6858	0.6057
Sb8	2010	11.8	0.5682	0.6349	0.531	0.5741
Sb9	4010	9.5	0.5835	0.4331	0.6438	0.4065
Sb10	4010	12.25	0.6135	0.9133	0.6525	0.5214

Table 5. Statistical results of coherence for left hand activity

Stats.	F3-F4	C3-C4	P3-P4	O1-O2
Mean	0.6823	0.6922	0.6811	0.6291
Std. Dev	0.1086	0.0801	0.1242	0.0515
Std. Err	0.0343	0.0253	0.0392	0.0163

Table 6. Statistical results of coherence for right hand activity

Stats.	F3-F4	C3-C4	P3-P4	O1-O2
Mean	0.6093	0.6561	0.6254	0.5941
Std. Dev	0.0867	0.1385	0.0887	0.0916
Std. Err	0.0274	0.0438	0.028	0.0289

Fig. 7 is the plot showing the comparison of coherence related to electrodes pair for left and right hand 4 motor execution, the maximum values of coherence related to the pair C3-C4 for both left and right-hands 5 motor execution. Where all the other electrode pairs have less coherence than C3-C4. The results are showing that all the subjects are conscious during all motor execution tasks; also it is found that the subjects are showing large values of coherence for C3-C4 electrode pair. All the active frequencies 2 are in alpha band i.e. (8-13 Hz) and are associated to motor execution. Where all the other electrode pairs 3 have less values of coherence during motor execution performed by the subjects, these results are similar as the results of previous study done for eye open and eye close EEG signals published by Almurshedi and Ismail (2014).

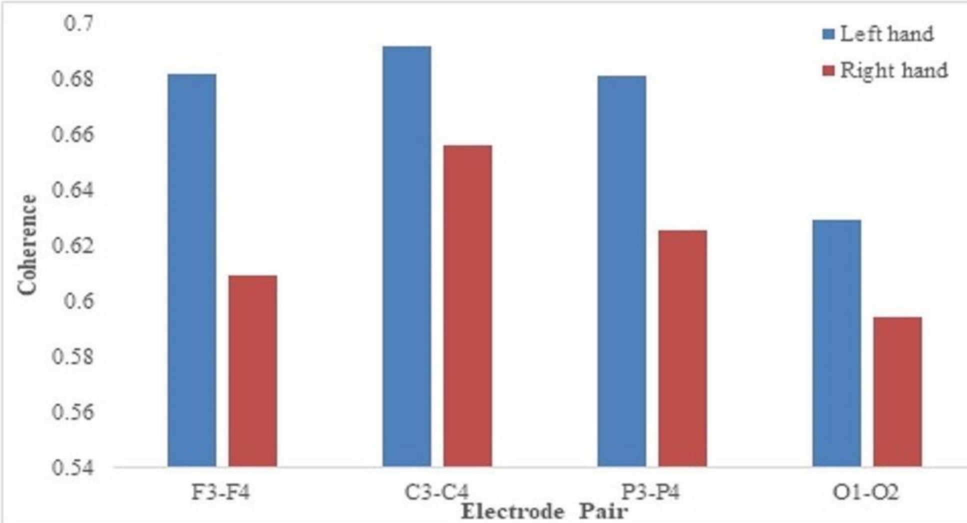

Fig. 7. Electrode pairs versus coherence graph for left and right hands activities.

Table 7. Phase for left and right hand motor execution between C3 and C4.

Subject	LH-Phase	RH-Phase
Sb1	-13.6	-98
Sb2	32.19	15.78
Sb3	-144	-115
Sb4	-15.14	-7.292
Sb5	-49.5	-129.3
Sb6	-134.2	123.3
Sb7	-109.3	-163.5
Sb8	-84	-67
Sb9	-38.34	-178.5
Sb10	-158.9	-10.69

Conclusion

According to the results of current study the active frequency for left-hand and right-hand motor execution performed by all subjects are showing frequency within alpha band, hence it is concluded that all the subjects are conscious, as suggested by earlier study (Banquet, 1973). It is also concluded that the coherence is maximum for electrode pair C3-C4, it is because the central motor cortex is responsible for all the motor executions Jerome and Donoghue (2000), where other electrode pairs are showing less values of coherence. From the analysis 70% of the subjects are showing phase locking values performed motor task is around 300 msec-500 msec, hence it is concluded that the brain regions become synchronized for this period. From these results the fact has been established that for 80% of the subjects the phase difference values are negative, with this it has been concluded that in case of left-hand motor execution the C4 is leading C3 and in case of right-hand motor execution C3 is leading C4, phase values of all the subjects for both left-hand and right-hand motor execution are given in Table 7. It is also found that phase differences are negative but varying values associated to different subjects in this study, further detail research is required to find the fact the behind varying negative phase difference.

Acknowledgments

Authors are thankful to the Department of Physics, University of Karachi for providing necessary facilities for conducting experiments. Authors are thankful to Dean Faculty of Science, University of Karachi for the financial assistance under DFS RESEARCH PROPOSAL GRANT 2017-2018 for EEG Motory and Cognitive study project.

Authors are also thankful to Department of Physics, Government National College, No.1 for providing their generous grants for the EEG equipment.

REFERENCES

Almurshedi, A. and A.K. Ismail (2014). Cross coherence independent component analysis in resting and action states EEG discrimination. *Journal of Physics: Conference Series*, 546(2014): 012019 DOI: 10.1088/1742-6596/546/1/012019

Andrew, M., H. David, P.F. Daniel and K. Peter (2017). EEG correlates of sensorimotor processing: Independent components involved in sensory and motor processing. . *Scientific Reports*, 7(1): 1-15.

Chaudhary, U., N. Birmbaumer and A.R. Murguialday (2016). Brain–computer interfaces for communication and rehabilitation. *Nature Reviews Neurology,* 12 (9): 513-525.

Delorme, A., M. Makeig, M. Fabre-Thorpe and T. Sejnowski(2002). From Single Trials EEG to Brain Area Dynamics. *Neurocomputing*, 44: 1056-1064.

Guger, C., W. Harkam, C. Hertnaes and G. Pfurtscheller(1999). Prosthetic Control by an EEG-based BrainComputer Interface. *AAATE 5th European Conference for the Advancement of Assistive Technology*, pp.3-6.

Handayani, N., F. Haryanto, S.N. Khotimah, I. Arif and W.P. Taruno (2018). Coherence and phase synchrony analyses of EEG signals in mild cognitive impairment(MCI). *Polish Journal of Medical Physics and Engineering*, 24(1): 1-9.

Helsinki (2001). World Medical Association Declaration of Helsinki. *Bulletin of World Health Organization*, 79(4).

Homan, R.W., J. Herman and P. Purdy (1987). Cerebral location of international 10-20 system electrode placement. *Electroencephalography and Clinical neurophysiology*. 66(4): 376-382.

Iriarte, J., E. Urrestarazu, M. Valencia, M. Alegre, A. Malanda *et al*. (2003). Independent Component Analysis as a Tool to Eliminate Artifacts in EEG: A quantitative study. *Journal of clinical neurophysiology*, 20(4): 249-257.

Jahangir, M., S.T.Iqbal, R. Rizwan, A.S. Nasir, S.M. Naqvi and Imran Siddiqui (2017). Spectral and Spatial Feature Extraction of Electroencephalographic. *Journal of Basic and Applied Sciences*, 13: 104-113.

Jerome, N.S. and J.P. Donoghue (2000). Plasticity and Primary Motor Cortex. *Annual Review of Neuroscience*, 23: 393-415.

Banquet, J.P. (1973). Spectral Analysis of the EEG in meditation. *Electroencephalography and Clinical Neurophysiology*, 35: 143-151.

Junfeng, S., H. Xiangfei and T. Shanbao (2012). Phase Synchronization Analysis of EEG Signals. *IEEE Transactions on Biomedical Engineering*, 59(8): 2254-2263.

Kroupi, E., A. Yazdani, J.M. Vesin and T. Ebrahimi (2013). EEG Correlares of Pleasent and Unpleasent Odor Preception. *ACM Transactions on Multimedia Computing Communications and Applications*, 2(3). 10.1145/2637287

Lebedev, M.A. and M.A. Nicolelis (2017). Brain-machine interfaces: From basic science to neuroprostheses and neurorehabilitation. *Physiological Review*, 97(2): 767-837.

Akin, M. (2002). Comparison of Wavelet Transform and FFT Methods in the Analysis of EEG Signals. *Journal of Medical Systems*, 26(3): 241-247.

McFarland, D.J., Jr. Wolpaw (2008). Brain-computer interface operation of robotic and prosthetic devices. *Computer*, 41: 52-56.

Nunez, P.L., R. Srinivasan, A.F. Westdorp, R.S. Wijesinghe, D.M. Tucker, R.B. Silberstein and P.J. Cadusch (1997). EEG coherency I: Statistics, reference electrode, volume conduction, Laplacians, cortical imaging, and interpretation at multiple scales. *Electroencephalography and Clinical Neurophysiology*, 103(5): 499-515.

Quiroga, R.Q., A. Kraskov, T. Kreuz and P. Grassberger (2002). Performance of different synchronization measures in real data: A case study on electroencephalographic signals. *Physical Review E*, 65(4). DOI: 10.1103/PhysRevE.65.041903

Reed, C.M.S. and S.J. Nasuto (2007). A novel approach to the detection of synchronisation in EEG based on empirical mode decomposition. *Journal of Computational Neuroscience*, 23(1): 79-111.

Ronak, B., Y. Sun, N. Helian and T. Steffart (2018). The Correlation between EEG Signals as Measured in Different Positions on Scalp Varying with Distance. *Procedia Computer Science*, 123: 92-97.

Sankari, Z. and H. Adeli (2011). Intrahemispheric, interhemispheric, and distal EEG coherence in Alzheimer's disease. *Clinical Neurophysiology*, 122(5): 897-906.

Sivakami, A. and S.S. Devi (2015). Analysis of EEG for motor imagery based classification of hand activities. *International Journal of Biomedical Engineering and Science*, 2(3): 11-22.

Stoykov, M.E. and S. Madhavan (2015). Motor priming in neurorehabilitation. *Journal of Neurologic Physical Therapy*, 39(1): 33-42.

Wang, L., X. Guo, J. Sun, Z. Jin and S. Tong (2012). Cortical networks of hemianopia stroke patients: A graph theoretical analysis of EEG signals at resting state. . *Annual International Conference of the IEEE Engineering in Medicine and Biology Society*, pp.49-52.

Wolpaw, J.R., N. Birbaumer and D.J. McFarland (2002). Brain–computer interfaces for communi cation and control. *Clinical Neurophysiology*, 113: 767-791.

Yang, L., L.L. Mei and L. Ke (2016). A multiwavelet-based time-varying model identification approach for time–frequency analysis of EEG signals. *Neurocomputing*, 193: 106-114.

(*Accepted for publication May 2020*)